Dynamic voltage stability of unbalanced DNs with high penetration of roof-top PV units

Monirul Islam[1], Mithulananthan Nadarajah[1], and M.J. Hossain[2]

[1]Power and Energy System group, School of ITEE, University of Queensland, Brisbane, Australia
[2]School of Electrical and Data Engineering, University of Technology, Sydney, Australia
mdmonirul.islam@uq.edu.au, mithulan@itee.uq.edu.au, Jahangir.Hossain@uts.edu.au

***Abstract*— Dynamic voltage instability (DVI) issue is one of the primary concerns in distribution networks (DNs) due to the growing integration of low-inertia compressor motor loads. Moreover, the inherent unbalanced nature of DNs as a result of unbalanced load could make the DVI issues more severe. Additionally, with the way rooftop photo-voltaic (PV) units, often in the form of single-phase units growing, DVI issues might be a threat to secure operation of DNs (both low and medium voltage) in the future. Though dynamic voltage stability (DVS) has been researched well in DNs, how imbalance would influence the issue yet to be fully understood, especially with growing PV units. It needs to be mentioned that although the roof-top PV units are connected to the low-voltage DNs, their impacts on the DVS can propagate to the immediate medium-voltage DNs. Hence, this paper systematically examines the impacts of imbalance on the DVS of medium-voltage DNs with high PV penetrations first. The degree of unbalance is defined, and then DVS is thoroughly investigated considering various unbalance scenarios. Two indices i.e. voltage nadir and rate of change of voltage recovery (ROCOVR) are proposed for clear understanding of the voltage dynamics at each phase. It is observed that the increment of system imbalance can significantly affect the DVS in a deprived way. Finally, this paper has discussed and compared mitigation strategies with respect to cost and DVS improvement. Case studies are conducted on two IEEE benchmark test systems, namely, IEEE 4 bus and IEEE 15 bus systems. It is revealed that reactive power injection by rooftop PV inverters would be the most cost-effective solution to avoid a probable instability while mitigating the impacts of imbalance.**

***Index Terms*— Dynamic voltage stability, Energy storage system, Fault ride-through, Photovoltaic systems, Transformerless inverters, Single-phase, Unbalance.**

I. INTRODUCTION

The necessity of clean and low-cost energy, owing to the apprehensions of environmental issues and swelling energy demand, has been leading the power systems to move towards renewable. It is to be noted that among many renewable energy technologies, the PV system is recognized as one of the fastest growing sources due to its availability, low maintenance cost, and most significantly declining overall energy cost [1]. Furthermore, due to the advancement of power electronics and government incentives for renewable energy, PV installations are growing rapidly all over the world. According to the newly published International Energy Authority report, worldwide installed capacity of PV power have reached a total of 500 GW in 2018 and forecasted to surpass 1.0 TW at the end of 2022 as illustrated in Fig. 1 [2]. While a number of utility scale PV plants are being installed worldwide, the contributions of single-phase small-scale, such as, roof-top type PV units which are generally being integrated into low-voltage DNs, in the overall capacity are significant [3]. As most of the roof-top type PV units are less than 10kW in size [4], the efficiency and reliability issues of these types of power generating units have become another concerns. Recently,

transformerless (TL) inverter technology has attracted enormous attention and is being integrated into the PV systems owing to its high efficiency and low-cost compared to their counterparts with transformer. Owing to the substantial penetration of single-phase TL-PV units, voltage instability issues of DNs have been receiving noteworthy interest both from academia and industry [5-7].

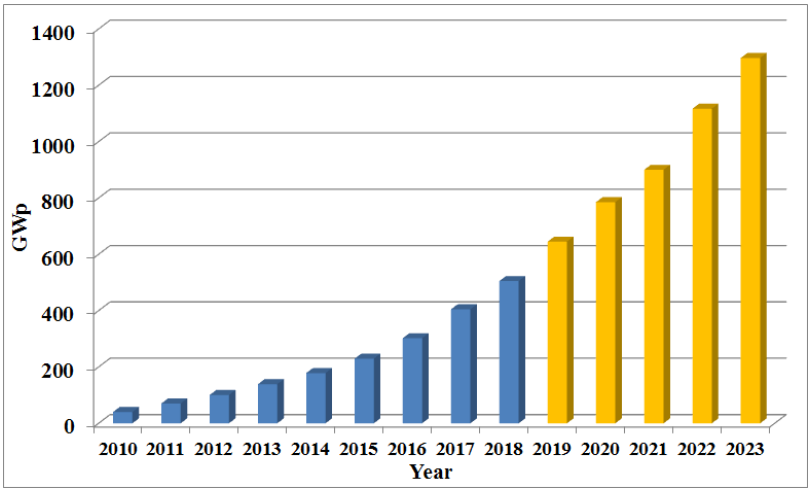

Fig 1. Worldwide installed capacity of PV power.

In 21st century, the world has experienced several blackouts, and voltage instability has played a role which could be partially or entirely in some of the blackouts [8, 9]. According to the complete "post-mortem," of the recent blackout occurred in South Australia, although the foremost cause was identified as frequency instability for the collapse, dynamic voltage instability which causes the disconnection of wind farm for violating the low-voltage ride-through (LVRT) requirement was reported as the initial reason [10]. It can be mentioned that dynamic voltage instability could be occurred due to several reasons. However, increased reactive power demand as a result of induction motor (IM) stall following a fault has been conceded to be the primary reason of DVI [8, 11]. Typically, an IM load draws 3-5 times of its rated current during stall period [12].

Dynamic voltage instability can be ensued either in short-term (several seconds) or long-term (seconds to minutes) time period scale [13]. It is worth to reveal that many studies have been conducted to contribute in better understanding of the long-term part of voltage instability caused by large PV integration [14-21]. In contrast, very few studies have focused on the short-term part of voltage stability which is also known as dynamic voltage stability [22-28]. In [22], the authors have investigated the impacts of LVRT by PV inverters on the DVS, and concluded that DVI is likely to be occurred in highly PV penetrated power systems after occurring a severe fault if the PV inverters are incapable of providing the LVRT. In [25], a new control strategy has been proposed to be implemented with PV units to improve the DVS. However, both of the studies [22, 25] are based on a transmission system where a balanced condition is considered. It is necessary to mention that the characteristics of DNs are dissimilar to high-voltage transmission systems due to several reasons, such as, high resistive to reactive (R/X) ratio, unbalanced load and line characteristics, unequal PV penetrations, etc. The authors in [24] have discussed the effects of PV power loss due to moving cloud and severe contingency on the DVS of DNs. It has been found-out that voltage instability can happen in a system with low voltage profile. In [23, 26], DVS of DNs has been investigated for different control strategies of

PV systems. Both papers [23, 26] have concluded that DVI is likely to occur with high PV penetration without LVRT capability, while it would be augmented with the reactive power support from PV systems. However, a balanced DN is considered in all studies [23, 24, 26], except few case studies are conducted in an unbalanced DN. Moreover, how unbalanced characteristics can affect the DVS of DNs have not been properly addressed and understood in all investigations [22-26].

The research presented in [7, 29-31] have discussed the effects of imbalance on the voltage stability. In [7], the authors have concluded that with the increment of imbalances, loadability of the system is decreased, and the transient stability margin is reduced. Although a dynamic voltage curve was employed (for the purpose of transient stability assessment), DVS was not investigated in [7]. The authors in [29] have shown that network's unbalance can be responsible for more critical voltage instability conditions. In order to assess the voltage stability of unbalanced distribution systems, a new technique has been proposed in [30] by taking into account the limit of reactive power generation. Ran et al presented a probabilistic evaluation of static voltage stability of an unbalanced distribution system considering wind power uncertainty in [31]. Though all papers [7, 29-31] have considered unbalanced system, the effects of unbalance characteristics on DVS of DNs have not been extensively examined.

From the prior discussion, it is noticeable that the power system can be adversely affected from the point of view of static voltage stability and transient stability due to the increased unbalances. However, to the best of author's knowledge, how the system is going to be affected in case of DVS have not been properly understood and addressed in the literature so far. Additionally, although the roof-top PV units are connected to the low-voltage DNs, their impacts on the DVS can propagate to the immediate medium-voltage DNs and to the transmission networks, which may lead to overall a system's voltage collapse. Therefore, a detailed analysis of DVS of DNs with high PV penetration considering system unbalance is required to better understand the systems' dynamic behavior following a contingency. Moreover, in order to mitigate any adverse impact; reliable, practical and economical solutions may become necessary while confirming the security. To bridge this gap, this paper aims to thoroughly investigate the effects of unbalance characteristics on the DVS of DNs, and provides reliable and cost-effective solutions to maintain systems' security. The key contributions of this study are summarized as below.

- The effects of uneven distribution of loads and single-phase PV units among phases of low-voltage networks on the DVS of medium-voltage DNs are critically examined. It is observed that in spite of unchanged load or PV penetrations on Phase B, DVS performance is degraded on this phase as unbalance increased. To be specific, when the VUF is increased to 2.54% and more, fault induced delayed voltage recovery (FIDVR) performance becomes very poor on Phase B in IEEE 4 bus system. In contrast, DVI is occurred for 3.8% VUF in IEEE 15 bus test system.
- As the system is unbalanced, to thoroughly understand the voltage dynamics and recovery scenarios on each phase, two new indices i.e. voltage nadir and ROCOVR are proposed. These indices showed that DVS on different phases of unbalanced DNs could be non-identical. It is expected that this index will assist the power system operators as well as researchers for better analysing the dynamics of voltage recovery at all phases in unbalanced networks.
- Finally, in order to alleviate the DVI, three remedial measures, such as (1) reactive power injection by TL-PV systems, (2) installation of battery energy storage system (BESS) and (3) distributed static VAR compensator (D-STATCOM) are suggested. It is shown that the DVI due to the increased imbalance can be alleviated by implementing the mitigation devices, although comparatively slower voltage-recovery can still be existent with the increment of imbalance.

Finally, reactive power support by roof-top PV systems is found to be the most cost-effective solution in mitigating probable instability.

The remaining of the paper is organized as follows: the TL-PV system including the LVRT control is developed in Section II, followed by the voltage unbalance and the methodology of DVS study in Section III. Case studies are conducted on modified IEEE 4 bus and IEEE 15 bus test systems, and the results are presented and discussed in Section IV. In order to improve DVS, mitigation measures are proposed and compared in Section V. Finally, Section VI accumulates the conclusions and contributions of this research.

II. Modelling of the PV Systems and Grid Requirements

A. *Modelling of the single-phase TL-PV inverter:*

Grid-tied PV systems generally include a transformer to provide galvanic isolation between PV panel and grid that can lead to lower-efficiency, higher-cost and bigger-size. It is therefore desirable to avoid transformer in the PV inverter; however, additional care must be taken to meet the safety requirement. Recently, TL-inverters have been invented for the PV systems which offer high-efficiency with low leakage current. In addition, it reduces the cost, size, and weight compared to their counterparts with a transformer. Several TL topologies have been proposed in the literature to increase the efficiency with reduced the leakage current [32-37]. The highest efficient topology that has been proposed in [32] is called highly efficient and reliable inverter concept (HERIC). However, due to the lack of clamping branch, high frequency common-mode voltage can be observed in HERIC topology, and hence leakage current may flow through the whole system. In order to completely reduce the leakage current, a six-switch based topology has been proposed in [37] with a capacitor divider diode clamping branch, which is called 'H6' topology. However, both of the topologies are proposed for unity power factor operation though a slight adjustment would allow them to control reactive power. In [36], another six-switch based 'H6-type' topology has been proposed. The main advantage of 'H6-type' topology is that it has been proposed with reactive power control capability. Therefore, in this paper, 'H6-type' topology is implemented for TL-PV application.

B. *Development of direct-quadrature based control:*

The voltage oriented control of current in the direct-quadrature (dq) reference frame is well known for three-phase grid-connected converters. Recently, this type of control is being implemented for single-phase applications [38, 39]. In this research, the conventional dq-based controller is employed, which include outer power control and inner current control loop as illustrated in Fig. 2. The instantaneous PV output power can be defined as follows:

$$\begin{bmatrix} P_{PV} \\ Q_{PV} \end{bmatrix} = \frac{1}{2}\begin{bmatrix} V_d & V_q \\ V_q & -V_d \end{bmatrix}\begin{bmatrix} I_d \\ I_q \end{bmatrix} \tag{1}$$

where P_{pv} and Q_{pv} are the active and reactive power delivered by PV, V_d, and I_d are the d-components, and V_q and I_q are the q-components of grid voltage and current. As the q component of grid-voltage is zero, instantaneous PV output power for single-phase system can be simplified as:

$$\begin{bmatrix} P_{PV} \\ Q_{PV} \end{bmatrix} = \frac{1}{2}V_m\begin{bmatrix} I_d \\ -I_q \end{bmatrix} \tag{2}$$

From (2), the reference active and reactive current in dq-frame can be determined as follows:

$$\begin{bmatrix} I_{drefPV} \\ I_{qrefPV} \end{bmatrix} = \frac{2}{V_m}\begin{bmatrix} P_{refPV} \\ -Q_{refPV} \end{bmatrix} \tag{3}$$

These current references are passed through a closed loop current controller to obtain final dq-axes references, where two PI based controllers have been implemented. Lastly, dq-axes voltages are transformed into αβ-reference frame to generate SPWM switching signals for the TL-inverters.

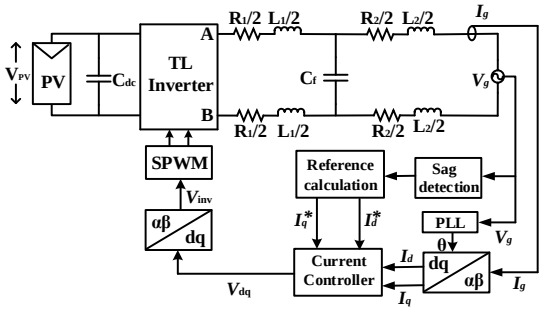

Fig 2. Overall control structure of TL-PV systems.

C. Low-voltage ride-through requirement:

Typically, the grid-tied inverters stop operation following a severe disturbance to protect itself from being damaged due to over-current. However, several grid-codes have recently been updated demanding grid-tied inverters to ensure LVRT capability instead of getting disconnected from the grid. As seen in Fig. 3, the LVRT requirements are dissimilar in different countries [40-42]. If the voltage drops below 20% for the duration of more than 15ms, the inverters should be disconnected from the grid which is identical for all presented countries. According to Japanese grid code, the converters are required to remain connected for 1.0s with the voltage drops to 20%, followed by the voltage recovery to 80% during next 0.2s. The converters are allowed to stay connected until 0.5s if the voltage level is kept at 20%, followed by the voltage recovery to 80% within 1.5s in the Spain. The German grid-code demands LVRT capability for the duration of 0.15s with the voltage level at 0% and next 0.35s with the voltage level at 30%, followed by the recovery of 90% within the period of 1.5s. Britain grid-code allows the inverter to continue operation if the voltage level doesn't fall below 15% for 0.16s (during fault) and then quickly recover to 95% within 0.5s (after the fault). It can be seen from Fig. 3 that Spain has imposed less strict LVRT requirement among them. Therefore, in this paper, Spanish LVRT instruction is taken into account to recognize whether the system will face any PV disconnection.

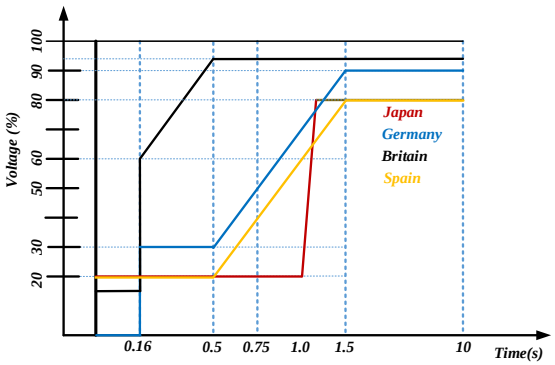

Fig 3. LVRT requirement for grid-connected converters in different countries [40-42].

III. VOLTAGE UNBALANCE FACTOR AND METHOD OF DVS STUDY

A. Voltage unbalance:

There are several reasons of voltage imbalance such as line configuration, unbalance loading, unequal PV penetrations in phases, etc. [43]. Thus considering a residential DN to be fully balanced might be impractical. However, as the electrical equipment are likely to be adversely affected by the voltage imbalance [44, 45], range of satisfactory voltage imbalance has been defined in many international standards. For instance, the International Electro-technical Commission have advised that voltage imbalance should not be surpassed a maximum of 2.0% [44]. Another standard ANSI C84.1-1995 have suggested that a maximum of 3.0% is acceptable with no load condition [44, 46]. The percentage voltage imbalance has been defined by the National Electrical Manufacturer Association as the ratio of maximum deviation from average to the average three-phase voltage [47]:

$$\%\ Volatge\ Unbalance = \frac{Maximum\ deviation\ from\ average}{Average\ of\ \ three\ phase-phase\ voltage} * 100 \tag{4}$$

However, in European standards, the degree of unbalance has been measured by using the index called voltage unbalance factor as is given in (5) [44].

$$\%\ VUF = \frac{V_N}{V_P} * 100 \tag{5}$$

where V_P is positive and V_N is the negative sequence voltages. The sequence voltages (V_P and V_N) can be determined using the symmetrical components as given in (6).

$$\begin{bmatrix} V_P \\ V_N \end{bmatrix} = \frac{1}{3}\begin{bmatrix} 1 & a & a^2 \\ 1 & a^2 & a \end{bmatrix}\begin{bmatrix} V_a \\ V_b \\ V_c \end{bmatrix} \tag{6}$$

where $a = e^{j120^o}$.

B. Methodology to study the dynamic voltage stability:

As the most common method of DVS study is the non-linear time-domain simulation (TDS) using the dynamic-model of the components in the networks, in this paper, TDS is carried-out first in the Matlab/SIMULINK software platform. Later, for further evaluation of the DVS in an unbalanced network, a modification of the index proposed in proposed in [48] called *transient voltage severity index (TVSI)* is developed and implemented. Furthermore, to better understand the voltage dynamics at each phase, two new indices: (1) voltage nadir and (2) ROCOVR is proposed. The details of the indices are given in the subsequent sections.

(i) Transient voltage severity index (TVSI): The index called TVSI was proposed considering a balanced network. However, in case of unbalanced system, the TVSI is required to be modified to accommodate unequal phase-voltage. In this paper, the modification is conducted by determining the TVSI at each phase according to (8) first. Note that higher TVSI value indicates weak DVS [48] performance. Consequently, to capture the deprived conditions of DVS among three phases, the maximum value of TVSI is taken. The modification of the TVSI would be as follows:

$$TVSI = \max(TVSI_A, TVSI_B, TVSI_C) \tag{7}$$

where $TVSI_A$, $TVSI_B$ and $TVSI_C$ are the *TVSI* of phase *A*, *B* and *C*, respectively, which are given in (8).

$$TVSI_{A,B,C} = \frac{\sum_{i=1}^{N}\sum_{t=T_c}^{T} TVDI_{A,B,C}^{i,t}}{N*(T-T_c)} \tag{8}$$

where N is the total number of buses, T and T_c are the considered transient time-frame and fault clearing time respectively, and $TVDI^{i,t}_{A,B,C}$ are the transient voltage deviation index for phase A, B and C. The $TVDI^{i,t}_{A,B,C}$ can be defined in (9).

$$TVDI_{A,B,C}^{i,t} = \begin{cases} \dfrac{V_{A,B,C}^{i,t} - V_{A,B,C}^{i,0}}{V_{A,B,C}^{i,0}} & \text{if} \quad \dfrac{V_{A,B,C}^{i,t} - V_{A,B,C}^{i,0}}{V_{A,B,C}^{i,0}} \geq \gamma \quad \Delta t \in [T_c, T] \\ 0 & \text{otherwise} \end{cases} \tag{9}$$

where $V^{i,t}{}_{A,B,C}$ are the phase voltages magnitude of bus i at time t, $V^{i,0}{}_{A,B,C}$ are the pre-fault phase voltages of bus i, Δt is step time, and γ is the threshold voltage.

(ii) Voltage nadir and rate of change of voltage recovery (ROCOVR): As discussed in the previous section, TVSI would capture the severity of overall DVS performance and can be used for comparison among different scenarios. However, different aspects of DVS such as how dip is the voltage during faults, how the post-contingency voltage is recovering, cannot be captured. Therefore, to dynamically capture different aspects of DVS, voltage nadir and ROCOVR are proposed. Similar to the frequency nadir, voltage nadir is defined as the minimum voltage as a results of a contingency. On the other hand, unlike rate of change of frequency, ROCOVR is introduced to examine the system's voltage recovery-speed. ROCOVR is the average of time derivative of the power system's voltage following a disturbance during a considered transient time frame (T). It needs to mention that higher value of ROCOVR means higher recovery speed so as enhanced DVS. ROCOVR can be calculated according to the following equation:

$$ROCOVR = \frac{T - T_c}{\Delta t} \sum_{t=T_c}^{T} \frac{d}{dt} V \quad \Delta t \in [T_c, T] \tag{10}$$

IV. Case Studies

In order to thoroughly understand the impact of imbalance on DVS of DNs, several case studies based on VUF are conducted on two IEEE test systems, namely, IEEE 4 bus and IEEE 15 bus test systems. Two types of scenarios are focused: (1) unbalanced loading and (2) unequal PV penetrations in different phases. It is assumed that the PV systems are consisting of the LVRT capability without reactive power support. As a three line to ground (3LG) fault is the most severe one, case studies are accomplished by triggering a 3LG fault at bus 1 for the duration of 0.2s.

A. Case studies on IEEE 4 bus system:

The IEEE 4 bus system is modified by including TL-PV systems and IM loads. A new transformer (Tr2) is installed at bus 4 as shown in Fig. 4, which creates a new bus (bus 5). The designed per unit parameters of Tr2 is same as that of transformers 1 (Tr1). The TL-PV systems and the IM loads are connected at bus 4 which is termed as point of common coupling (PCC). It may be noted that IM load could be as high as 75% of total load in a residential DN during a hot day in summer though it can vary depending on the region [12, 49]. As the IEEE 4 bus system represent a DN, 70% loads are modelled as IM load. The modified loads of IEEE 4 bus system and the per unit parameters of IM loads are given in Table A1 and Table A2, respectively in appendix A. For this study, the short circuit capacity (SCC) of the system is considered to be 83 MVA, while the X/R ratio is 6.0. The penetration level of PV power is computed according to (11).

$$PV\ Penetration\ Level = \frac{Injected\ PV\ Power}{Total\ Load} * 100 \tag{11}$$

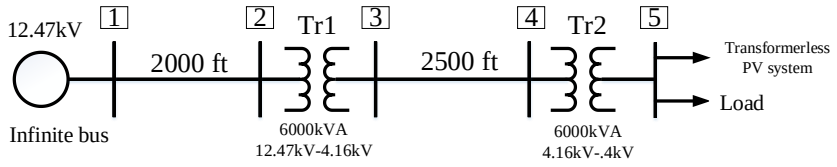

Fig 4. Modified IEEE 4 bus system.

(i) Impact of unbalanced loading: In order to create voltage imbalance, it is assumed that total load is S_L, and phases A, B and C are connected with $S_L/3/(1+\alpha)$, $S_L/3/(1+\beta)$ and $S_L/3/(1+\gamma)$ pu respectively. It may be noted that the values of α, β and γ are real and very small for practical power systems. It is found that in case of transmission networks, the values of α, β and γ are negligible as unbalance is hardly existed, while in case of DNs, these values are kept very less (roughly less than 0.2) to reduce the unbalance among phases [7, 50, 51]. The investigated cases are presented in Table 1, where the VUF in Case 1 is 0.15% which is increased to 3.08% in Case 5. Witnessed by Table I, β is always zero which means that the load has been unchanged on phase B.

Table I: Investigation cases for unbalanced loading

Cases	α	β	γ	VUF (%)	LVRT Capability	PV Penetration	Reactive power support
1	0	0	0	0.15	Yes	50%	No
2	-0.048	0	0.048	0.81			
3	-0.087	0	0.087	1.72			
4	-0.133	0	0.133	2.54			
5	-0.161	0	0.161	3.08			

The dynamic phase voltages at PCC for unbalanced loading are shown in Fig. 5. It can be observed from Figs. 5(b) and (c) that the DVS is likely to be degraded as unbalanced increases. To be specific, the system has experienced the DVI on phase C in all cases except Case 1 as expected owing to the large loads. In contrast, Figs. 5(a) evidently indicates the augmentation of DVS while unbalance increases. This was predictable due to improved voltage profile on phase A as load decreased with the increment of VUF. However, an interesting observation is that even though the loads on phase B is kept constant, impaired DVS is noticeable with the increment of imbalance. The possible reasons of this weakened DVS could be the neutral point shifting as well as high losses in IM loads when unbalance increases, which are

comprehensively explained in Section IV(C). According to Spanish LVRT requirement which is the most flexible among regulations presented in Section II(C), grid-connected PV systems should be disconnected if PCC voltage does not come back to 80.0% of rated within 1.5s of the fault occurrence. It is perceived that voltage on phase C fails to reach to 0.8 pu in Cases 2, 3, 4 and 5, while it happens only in Case 5 for phase B. Accordingly, the TL-PV systems would be disconnected in those circumstances which may add an extra burden in DN.

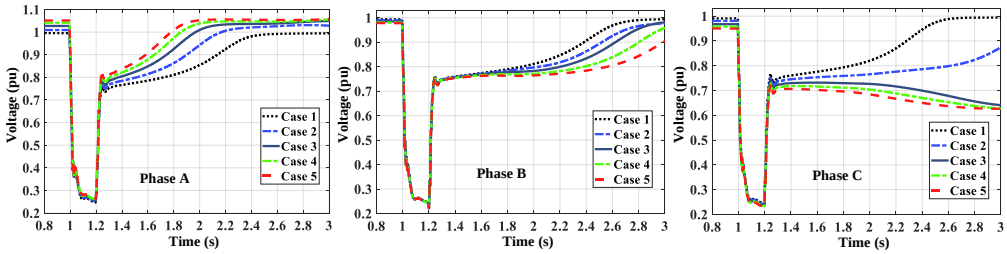

(a) (b) (c)

Fig 5. Excursion of voltage at PCC: (a) Phase A (b) Phase B and (c) Phase C with unbalanced loading.

(ii) Impact of unequal PV penetrations: To comprehensively investigate the impact of unequal PV penetrations on DVS, five cases are created by connecting unequal PV units at different phases. Table II demonstrates the cases, where increased PV penetration on phase A and the opposite on phase C is noticeable. However, the PV penetration on phase B is kept unchanged for all cases. As a result of this unequal PV penetrations, VUF increases from 0.15% in Case 1 to 3.80% in Case 5.

Table II: Investigation cases for unequal PV penetrations in IEEE 4 bus

Cases	Per Phase PV Penetration (%)			VUF (%)	LVRT Capability	Reactive power support
	Phase A	Phase B	Phase C			
1	50.00	50.00	50.00	0.15	Yes	No
2	55.55	50.00	44.44	0.96		
3	61.11	50.00	38.88	1.88		
4	66.67	50.00	33.33	2.82		
5	72.22	50.00	27.77	3.80		

The excursions in voltage at PCC subjected to the 3LG fault with unequal PV penetration are depicted in Fig 6. As can be seen, DVS is improved on phase A, while it has become weaker with the increment of imbalance on phase C. Consequently, DVI is occurred in Cases 3 to 5 on phase C. This is predictable due to PV power variation. However, voltage recovery-speed to pre-fault value on phase B is decreased for Cases 1 to 5 respectively although the number of PV units at this phase is same for all the cases. Unlike unbalanced loading, the DVI is occurred on phase B in cases 4 and 5. As observed, the voltage dynamics are very similar for unbalanced loading and unequal PV penetration in spite of the instability on phase B in Cases 4 and 5. It is understood that the possible reasons would be identical to the unbalanced loading.

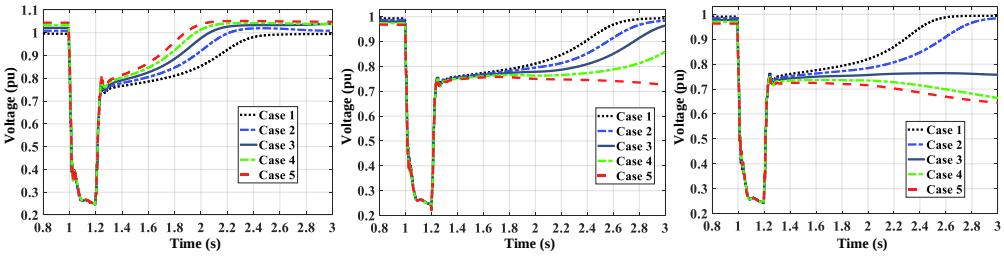

(a) (b) (c)

Fig 6. Excursion of voltage at PCC: (a) Phase A (b) Phase B and (c) Phase C with unequal PV units at different phases.

(iii) Index based assessment:

Voltage Nadir and ROCOVR: In order to quantify the severity of DVI in each phase, voltage nadir and ROCOVR for both scenarios are calculated and depicted in Figs. 7 and 8, respectively. It can be seen from Fig. 7(a) that voltage nadir on phase A for unbalanced loading is improved with the increment of imbalance, whereas it has been kept identical on phase B and impaired on phase C as expected. In contrast, no variation of voltage nadir is observed for unequal PV penetrations. However, as seen in Fig. 8, ROCOVR is gradually decreased on phases B and C for the cases 1 to 5 respectively in both scenarios, clearly indicates the weaken DVS as VUF increases. It can also be seen that phase A has been realized higher ROCOVR with the increment of imbalance, which is due to the low load or large PV units on this phase.

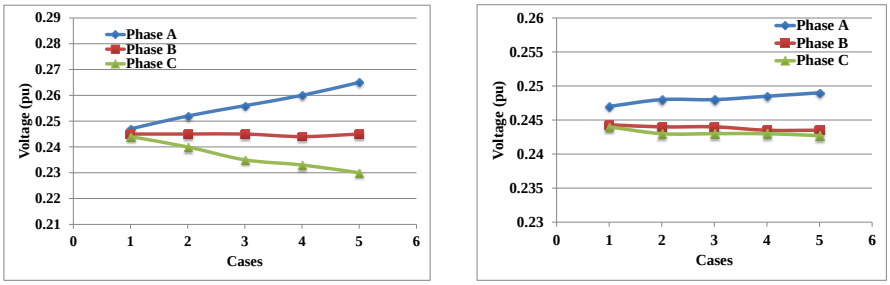

(a) (b)

Fig 7. Voltage nadir in different cases for: (a) unbalanced loading and (b) unequal PV penetrations.

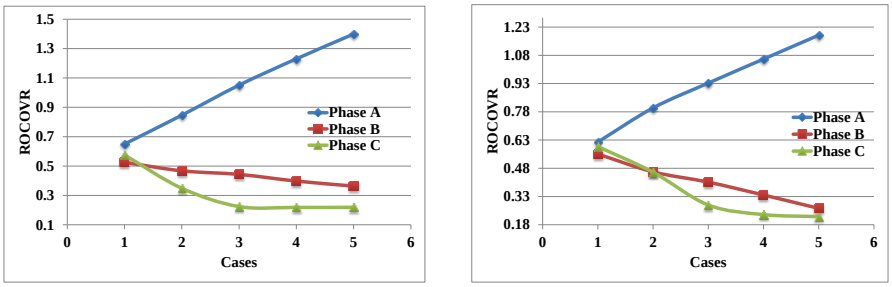

(a) (b)

Fig 8. ROCOVR in different cases for: (a) unbalanced loading and (b) unequal PV penetrations.

Calculation of TVSI: The index TVSI is computed for unbalanced network for all cases according to (7), and presented in Table III as well as depicted in Fig. 9. Throughout the calculation, the parameters are set as follows: *N=5, T=2s, T_c=1.2s, step time=20μs,* and *γ=20%*. It can be seen that TVSI values are gradually increased for the cases 1 to 5 with the increment of imbalance. To be specific, TVSI increase 253.85% and 224.95% when VUF rises 0.15% to 3.08% with unbalanced loading, and 0.15% to 3.80% with unequal PV units. As higher TVSI indicates impaired DVS, it can be concluded that DVS would be affected in a deprived way with the increment in imbalance.

Table III: TVSI for different cases presented in Table I.

Cases		Case 1	Case 2	Case 3	Case 4	Case 5
TVSI	Unbalanced loading	1675	3275	5314	5667	5927
	Unequal PV	1675	2223	4438	5095	5443

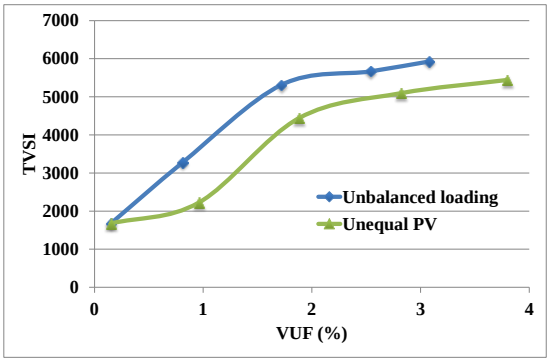

Fig 9. TVSI with the increment of VUF.

B. Case studies on IEEE 15 bus test system:

In this section, the case studies are carried out on a larger test systems i.e. IEEE 15 bus to further verify conclusions drawn on the voltage dynamics on an IEEE 4 bus system. The details of the IEEE 15 bus system can be found in [52, 53]. The PV systems are connected on nodes 3, 5 and 13 as shown in Fig. 10 to achieve total 50.0% penetration. As this test system can reflect a residential network, almost 60% IM loads have been accommodated that forms the load combination 60% IM-type and 40% ZIP-type. The modified loads are

given in Table A3 in Appendix A. The SCC of the network is designed to be 6.0. As can be seen in Fig. 10, node 13 is the most remotely located and delivering large loads. Therefore, the voltage dynamics at node 13 is observed subjected to a 3LG to thoroughly investigate the impact of imbalance on the DVS.

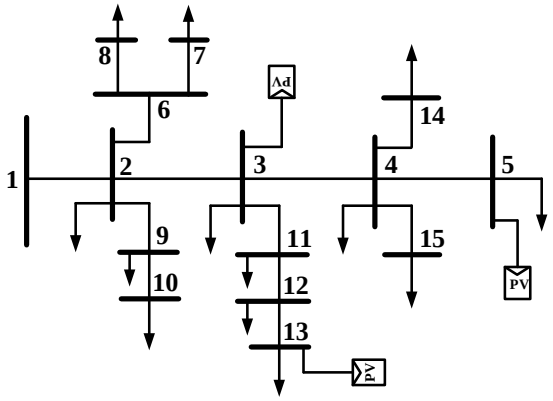

Fig 10. Modified IEEE 15 bus test system.

(i) Impact of unbalanced loading: The unbalance voltage is generated through changing the loads between the phases A and C. In this scenario, loads on phase C is increased, whereas phase A has realized the reduction of same quantity. As a result of load shifting, VUF is increased from 0.05% in Case 1 to 3.37% in Case 4. The details of VUF with the cases are given in Table IV.

Table IV: Investigation cases for unbalanced loading in IEEE 15 bus.

Cases	VUF (%)	LVRT Capability	Reactive power support
1	0.05	Yes	No
2	1.03		
3	2.17		
4	3.37		

The excursion in voltage at node 13 with the increment of VUF after a 3LG fault is illustrated in Fig. 11. As can be observed, owing to the decrement of load on phase A for the Cases 1 to 4 respectively, voltage recovery-speed to pre-fault condition is increased at the same order. In contrast, DVI in Cases 3 and 4, and delayed recovery in Case 2 can be perceived on phase C, which is very likely due to the increment of loads. However, witnessed by Fig. 11(b), declined voltage recovery-speed on phase B is noticed with the increment in VUF although the loads on phase B were kept unchanged. This observation is very identical to the voltage dynamics of phase B in IEEE 4 bus system presented in Fig. 5.

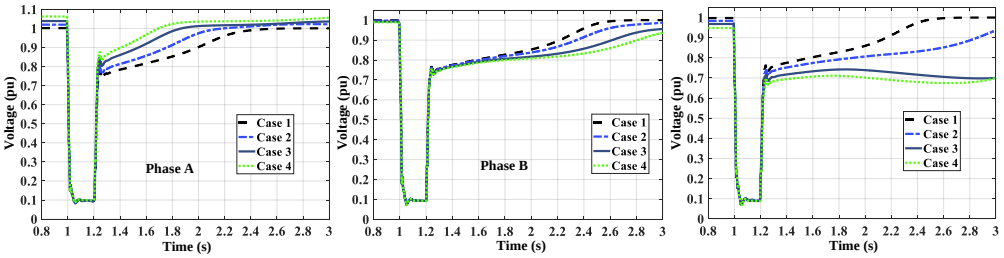

(a) (b) (c)

Fig 11. Excursion of voltage at node 13: (a) Phase A (b) Phase B and (c) Phase C for unbalanced loading.

(ii) Impact of unequal PV penetrations: Like an IEEE 4 bus system, scenarios to study the impact of an unequal PV penetration on the DVS are created by shifting the PV units of phase C into phase A, while the penetration on phase B is kept constant. As a result, the voltage profile on phase A is likely to increase, although phase C experiences a drop. Consequently, the VUF increases from 0.05% in Case 1 to 3.94% in Case 4. The per-phase PV power and the VUF for each case are given in Table V.

Table V: Investigation cases for unequal PV penetrations in IEEE 15 bus.

Cases	Per Phase PV Power (kW)			VUF	LVRT	Reactive power
	Phase A	Phase B	Phase C	(%)	Capability	support
1	300.0	300.0	300.0	0.05	Yes	No
2	400.0	300.0	200.0	1.28		
3	500.0	300.0	100.0	2.67		
4	600.0	300.0	00.00	3.94		

The dynamic voltage profile at node 13 is illustrated in Fig. 12 with unequal PV penetrations at different phases. It is clear that DVS on phase A is enhanced, whereas phase C is likely to realize a DVI in Cases 3 and 4 as expected. Furthermore, in spite of unchanged PV penetration, voltage retrieval speed is decelerated for the cases 1 to 5 on phase B. Therefore, the conclusions drawn on voltage dynamics after a fault due to the unequal PV penetrations from the case studies on IEEE 4 bus system are further verified in IEEE 15 bus test system.

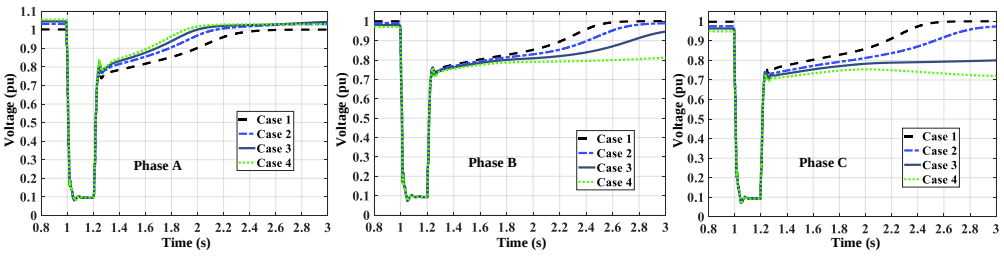

(a) (b) (c)

Fig 12. Dynamic voltage profile at bus 13: (a) Phase A (b) Phase B and (c) Phase C for with unequal PV units at different phases.

C. Analysis and discussion:

It is very challenging to identify the actual parameters which are contributing in delayed voltage recovery with the increase in imbalance. It is believed that a number of parameters are responsible for weakened DVS. However, two key reasons are identified and explained in this paper: (1) high losses in IM load with

increased imbalances and (2) the coupling among phases. It has been concluded in [54, 55] that the greater the negative and zero sequence component, the more the losses in IM loads. In the event of DVS, VUF increases following a contingency due to different loading conditions and voltage drop which in results increased losses and delayed recovery. For better understanding, IEEE 4 bus system has been simplified considering only bus 1 and 2. Therefore, the simple two bus system can be characterized by (12) [56].

$$\begin{bmatrix} \vec{V}_{2a} \\ \vec{V}_{2b} \\ \vec{V}_{2c} \end{bmatrix} = \begin{bmatrix} \vec{V}_{1a} \\ \vec{V}_{1b} \\ \vec{V}_{1c} \end{bmatrix} - L_{Length} \cdot \begin{bmatrix} \vec{Z}_{aa} & \vec{Z}_{ab} & \vec{Z}_{ac} \\ \vec{Z}_{ba} & \vec{Z}_{bb} & \vec{Z}_{bc} \\ \vec{Z}_{ca} & \vec{Z}_{cb} & \vec{Z}_{cc} \end{bmatrix} \cdot \begin{bmatrix} \vec{I}_a \\ \vec{I}_b \\ \vec{I}_c \end{bmatrix} \tag{12}$$

Note that the diagonal and off-diagonal elements of the line impedance matrix and the phase current are unequal under unbalanced conditions. Consequently, line voltage drop can be defined in (13) for unbalanced conditions [43].

$$\begin{bmatrix} \vec{\Delta V}_a \\ \vec{\Delta V}_b \\ \vec{\Delta V}_c \end{bmatrix} = L_{Length} \cdot \begin{bmatrix} \dfrac{\vec{Z}_{aa} \times \vec{I}_a + \vec{Z}_{ab} \times \vec{I}_b + \vec{Z}_{ac} \times \vec{I}_c}{\vec{I}_a} \times \vec{I}_a \\ \dfrac{\vec{Z}_{ba} \times \vec{I}_a + \vec{Z}_{bb} \times \vec{I}_b + \vec{Z}_{bc} \times \vec{I}_c}{\vec{I}_b} \times \vec{I}_b \\ \dfrac{\vec{Z}_{ca} \times \vec{I}_a + \vec{Z}_{cb} \times \vec{I}_b + \vec{Z}_{cc} \times \vec{I}_c}{\vec{I}_c} \times \vec{I}_c \end{bmatrix} \tag{13}$$

It is clear from (13) that voltage drops in phases will be different in unbalanced condition which depends on the current of each phase. As a result, the system will become more unbalanced following a disturbance due to different loading conditions which might be one of the causes of delayed phase voltage recovery.

In order to analyse the effect of coupling among phases on the DVS, voltage drop sensitivity to phase loading changes are calculated and plotted in Fig. 13. Original balanced load of IEEE 4 bus systems is considered as base case (1.0 pu) to calculate the sensitivity. It is clear that an increase in phase A or B or C loading level can cause significant voltage drop at the same phase which is expected. However, the most interesting observation is that it can affect other phases, such as, voltage drop in phase B is reduced due to a rise in phase A loading, while phase C is hardly affected. This is mainly happened due to the neutral point shifting as a result of variations in load or power injection in single-phase [12, 57, 58]. Identical trend is observed for an increment in loading in phases B and C as shown in Figs. 13(b) and (c), respectively. As voltage drop in one phase could be affected owing to the change of phase loading in an another phase, which can cause due to an increased imbalance following a severe contingency.

Commented [JH1]: Not a good sentence

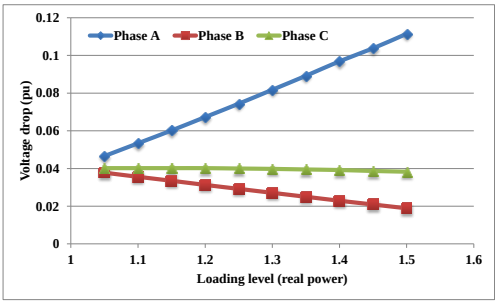

(a)

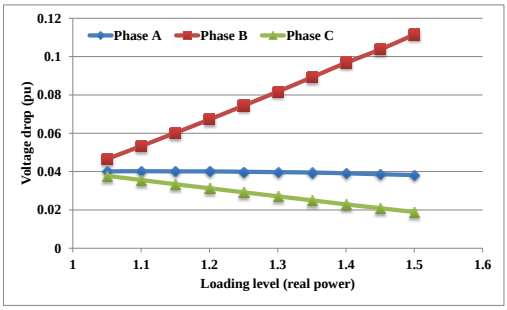

(b)

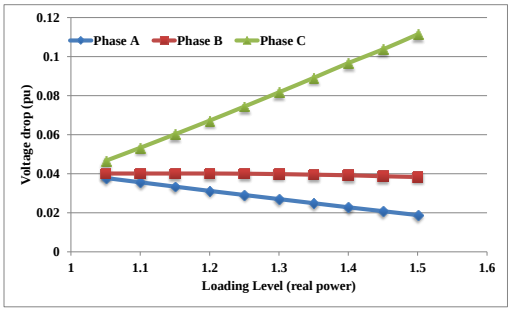

(c)

Fig 13. Voltage drop sensitivity with loading variation in: (a) phase A (b) phase B and (c) phase C.

V. Potential Solutions

According to the prior investigations, the networks might experience a DVI when unbalance increases. Consequently, some potential solutions are required to maintain the system's security. As the instability problems are due to the increased imbalance in this case, the most cost-effective solutions would be rearranging PV units and loads among phases, and maintain the networks in balanced conditions. However, in practical, it might not be possible to install equal loads and PV units among phases while considering different types networks and customers. Furthermore, several studies and operational planning are obligatory to recognize the effectiveness of this method which needs to be carried out in the planning stage. Therefore,

assuming the practical networks could be unbalanced and a solution is required, in this section, different types of approaches to mitigate DVI are discussed and compared to identify the potential one.

There are several methods to improve the DVS in unbalanced DNs, for example, partial load shedding, reactive power injection from roof-top PV systems, planning and implementation of D-STATCOM and/or BESS, etc. Though a number of researches have been conducted to ensure effective load shedding during a severe contingency [59, 60], it is not an attractive solution as the customers might not be pleased due to their load cut. In contrary, reactive power injection by roof-top PV inverters or deployment of BESS and/or D-STATCOM could be an efficient solution as load shedding can be avoided through this method. It is to be mentioned that while the large and medium scale PV plant are required to provide reactive power support, it is not essential for small-scale PV plants such as roof-top type. Therefore, performance of reactive-power injection from roof-top TL-PV inverters and installation of BESS and/or D-STATCOM are investigated with respect to DVS improvement. As the voltage dynamics due to increased imbalance after a disturbance is almost identical for unequal PV and unbalanced loading, in the following section, mitigation strategies are validated and compared only for unequal PV penetrations on IEEE 4 bus test system.

Commented [JH2]: Two sentences are contradictory

A. Reactive-power injection from roof-top TL-PV inverters:

Recently, a number of grid-codes have been restructured incorporating the requirements of reactive-power regulation proficiency by power electronics based renewable energy sources i.e. PV systems [41, 61-63]. However, in most of the grid-code, specific reactive power injection requirement by small-scale PV units (<10kW) has not been mentioned. Reactive power injection by roof-top type PV inverters could improve the DVS of DNs which is assessed in this section. The strategy for reactive power injection is designed following the German grid code (E.ON), where rated reactive current to be injected into the grid when the voltage drives underneath 0.5 pu [41]. The injected reactive current into grid through the TL-PV systems can be defined as follow:

$$\begin{cases} I_q = \mu(1-V_{gp})I_n & when \;\; 1-1/\mu \le V_{gp} \le 0.95 \\ I_q = I_n & when \;\; V_{gp} < 1-1/\mu \end{cases} \tag{14}$$

where V_{gp}, I_n and I_q are the per unit grid-voltage, rated-current of the TL-inverter and delivered reactive-current, respectively. Here μ is introduced for derating operation which is as:

$$\mu = \frac{\left(I_q - I_{qo}\right)/I_n}{(1-V_{gp})} \tag{15}$$

where I_{qo} is the primary reactive-current before the contingency, which is set to zero assuming that the roof-top PV units function at unity power-factor when there is no fault (*0.95 <= V_{gp} <= 1.05)*. According to (14), injected reactive-current is computed for various values of μ and plotted in Fig. 14. As can be perceived, injected reactive-current would be reduced with the decrement of μ. In this paper, to realize comparatively large injection of reactive-current with less grid-voltage dip, μ is chosen to be 3.0.

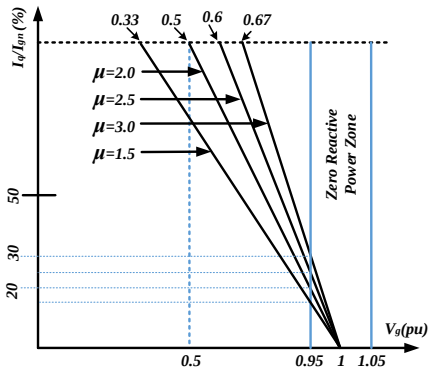

Fig 14. Variation of reactive-current for several values of μ.

The efficacy of reactive-power support by TL-PV inverters to alleviate any instability due to imbalance is explored through non-linear simulations, and compared by calculating indices for the cases presented in Table II. Figure 15 depicts the dynamic voltage profile at PCC, designate that post-contingency voltage recovery to pre-fault value has been ensured in all phases, mitigating the effects of imbalance on DVS. This is happened due to reactive-power provision of TL-PV inverter as shown in Fig. 16. It can be seen that TL-PV systems inject reactive power during fault whilst it is reduced gradually with the increment of voltage. Furthermore, reactive power support on phase A and C varies for different cases which are due to the dissimilar voltage conditions. In contrast, almost identical reactive power is injected on phase B as seen in Fig. 15(b). It is also noticeable that phase voltages have returned to 0.8 pu within 1.5s of fault occurred. Therefore, according to Spanish LVRT requirement described in Fig. 3, the system should be capable of avoiding any PV power loss.

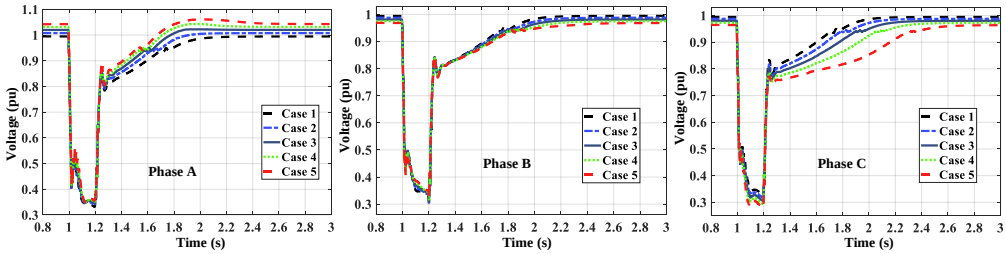

(a) (b) (c)

Fig 15. Dynamic voltage profile at PCC with reactive power support by TL-PV inverters: (a) Phase A, (b) Phase B and (c) Phase C.

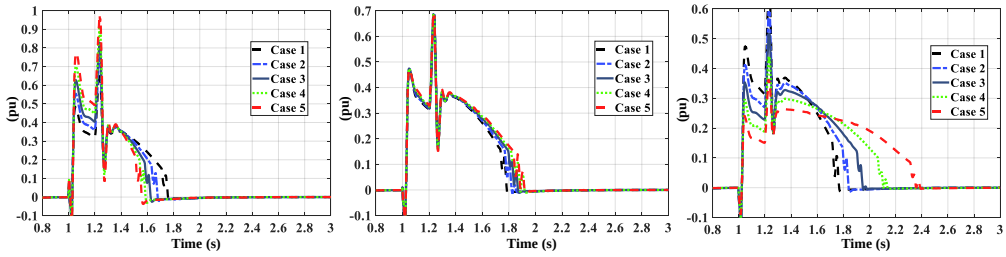

(a) (b) (c)

Fig 16. Reactive-power delivered by TL-PV systems on: (a) Phase A, (b) Phase B and (c) Phase C.

The voltage dynamics of the network at each phase has been investigated by calculating the voltage nadir and ROCOVR as given in Fig. 17. It can be observed that phases A and B comprehend the improvement in voltage nadir, while phase C has seen the opposite with the increment of imbalance. On the other hand, ROCOVR is improved only on phase A which was expected owing to higher voltage profile. However, the ROCOVR is declined on phases B and C, designates that the system can still realize slow-recovery due to the increased imbalance despite reactive power support from TL-PV inverters that helps to mitigate the DVI.

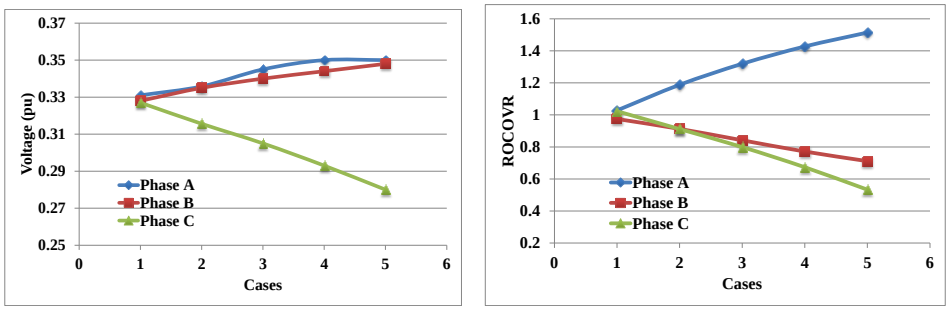

(a) (b)

Fig 17. (a) Voltage nadir and (b) ROCOVR with reactive power support from TL-PV inverters.

The TVSI is calculated for this scenario and presented in Table VI. A rise in TVSI can be observed with the increment in imbalance in Cases 1 to 5 respectively, which is owing to unequal PV and voltage profile in phases B and C. As seen in the prior section with ROCOVR, it can also be observed from TVSI that increased imbalance could affect the recover-speed in a deprived way although instability is alleviated through reactive power support. Finally, the reduction of TVSI is very much notable; for example, the TVSI in Case 1 with reactive power support is 94.5% less than TVSI in Case 5 without support.

Table VI: TVSI with reactive power support by TL-PV inverter.

Cases		Case 1	Case 2	Case 3	Case 4	Case 5
TVSI	Without reactive power support	1675	2223	4438	5095	5443
	With reactive power support	301	303	458	714	1083
Percentage reduction		82.1	86.4	89.7	85.95	80.1

B. Installation of BESS and/or D-STATCOM:

In this section, the effectiveness of installing a BESS and/or D-STATCOM in alleviating the DVI is investigated. As the system is unbalanced, the detail dynamic model of the BESS and/or D-STATCOM is developed based on the sequence components. According to three-phase basic power theory, instantaneous active and reactive power can be calculated using (16).

$$\begin{bmatrix} p \\ q \end{bmatrix} = \frac{3}{2} \begin{bmatrix} v_\alpha & v_\beta \\ v_\beta & -v_\alpha \end{bmatrix} \begin{bmatrix} i_\alpha \\ i_\beta \end{bmatrix} \quad (16)$$

In case of an unbalanced condition, power components in (16) can be rewritten as:

$$\begin{bmatrix} p \\ q \end{bmatrix} = \begin{bmatrix} p^{+} \\ q^{+} \end{bmatrix} + \begin{bmatrix} p^{-} \\ q^{-} \end{bmatrix} + \begin{bmatrix} \tilde{p} \\ \tilde{q} \end{bmatrix} \tag{17}$$

where p^{+}, p^{-} and q^{+}, q^{-} are the positive and negative sequence instantaneous active and reactive power, respectively, and $\tilde{p}$ and $\tilde{q}$ are the oscillating terms at twice the grid frequency. The power components in (17) can be calculated as a function of voltage and current in synchronous reference frame (SRF) as follows [64]:

$$p^{+} = \frac{3}{2}\left(v_{\alpha}^{+} i_{\alpha}^{+} + v_{\beta}^{+} i_{\beta}^{+}\right) \tag{18}$$

$$p^{-} = \frac{3}{2}\left(v_{\alpha}^{-} i_{\alpha}^{-} + v_{\beta}^{-} i_{\beta}^{-}\right) \tag{19}$$

$$q^{+} = \frac{3}{2}\left(v_{\beta}^{+} i_{\alpha}^{+} - v_{\alpha}^{+} i_{\beta}^{+}\right) \tag{20}$$

$$q^{-} = \frac{3}{2}\left(v_{\beta}^{-} i_{\alpha}^{-} - v_{\alpha}^{-} i_{\beta}^{-}\right) \tag{21}$$

$$\tilde{p} = \frac{3}{2}\left(v_{\alpha}^{+} i_{\alpha}^{-} + v_{\beta}^{+} i_{\beta}^{-} + v_{\alpha}^{-} i_{\alpha}^{+} + v_{\beta}^{-} i_{\beta}^{+}\right) \tag{22}$$

$$\tilde{q} = \frac{3}{2}\left(-v_{\alpha}^{+} i_{\beta}^{-} + v_{\beta}^{+} i_{\alpha}^{-} - v_{\alpha}^{-} i_{\beta}^{+} + v_{\beta}^{-} i_{\alpha}^{+}\right) \tag{23}$$

where v_{α}, v_{β} and i_{α}, i_{β} are the point of coupling voltages and injected grid currents in SRF, respectively, and superscripts '+' and '–' designate the positive and negative sequence components. From (18)-(23), the active and reactive current components can be formulated as follows [64-66]:

$$\begin{bmatrix} i_{\alpha(p)} \\ i_{\beta(p)} \end{bmatrix} = \frac{2}{3}\frac{P^{+}}{\left(v_{\alpha}^{+}\right)^{2} + \left(v_{\beta}^{+}\right)^{2}}\begin{bmatrix} v_{\alpha}^{+} \\ v_{\beta}^{+} \end{bmatrix} + \frac{2}{3}\frac{P^{-}}{\left(v_{\alpha}^{-}\right)^{2} + \left(v_{\beta}^{-}\right)^{2}}\begin{bmatrix} v_{\alpha}^{-} \\ v_{\beta}^{-} \end{bmatrix} \tag{24}$$

$$\begin{bmatrix} i_{\alpha(q)} \\ i_{\beta(q)} \end{bmatrix} = \frac{2}{3}\frac{Q^{+}}{\left(v_{\alpha}^{+}\right)^{2} + \left(v_{\beta}^{+}\right)^{2}}\begin{bmatrix} v_{\beta}^{+} \\ -v_{\alpha}^{+} \end{bmatrix} + \frac{2}{3}\frac{Q^{-}}{\left(v_{\alpha}^{-}\right)^{2} + \left(v_{\beta}^{-}\right)^{2}}\begin{bmatrix} v_{\beta}^{-} \\ -v_{\alpha}^{-} \end{bmatrix} \tag{25}$$

where P and Q are the active and reactive power reference, respectively. Two control gains i.e. active k_p and reactive k_q are introduced as given in (26) to realize flexible active and reactive power injection [67].

$$k_p = P^{+}/P, \qquad k_q = Q^{+}/Q \tag{26}$$

Finally, the positive and negative sequence active (I_p) and reactive (I_q) reference current can be defined as [64]:

$$I_p^{+} = \frac{2}{3}\frac{k_p P}{V^{+}} \tag{27}$$

$$I_p^- = \frac{2}{3}\frac{(1-k_p)P}{V^-} \tag{28}$$

$$I_q^+ = \frac{2}{3}\frac{k_q Q}{V^+} \tag{29}$$

$$I_q^- = \frac{2}{3}\frac{(1-k_q)Q}{V^-} \tag{30}$$

In this investigation, 1000 kVA rated BESS and D-STATCOM are installed and connected at bus 4. In order to recognize the competency of BESS and D-STATCOM in voltage recovery at the same environment for the cases presented in Table II, it is assumed that both BESS and D-STATCOM are providing zero output power during normal grid condition (*0.95 <= V_{gp} <= 1.05*). However, when the system is encountered a contingency, BESS delivers only active power and D-STATCOM support the voltage by injecting reactive power. The control gains k_p and k_q are carefully chosen depending on the fault characteristics as follows:

$$\frac{k_{p,q}}{1-k_{p,q}} = \frac{V_{nom} - |V^+|}{VUF * |V^-|} \tag{31}$$

where V_{nom} is the nominal grid voltage before fault, V^+ and V^- are the amplitude of the positive and negative sequence grid voltage.

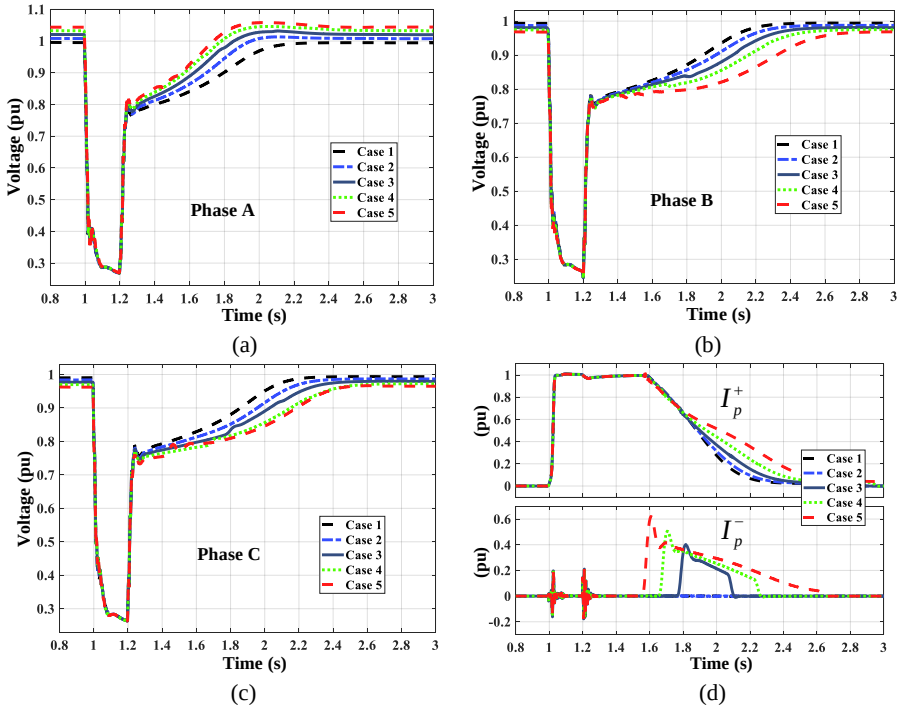

Fig 18. Dynamic voltage profile at PCC with BESS at bus 4: (a) Phase A (b) Phase B and (c) Phase C, and (d) Power delivered by BESS.

The dynamic response of the system's voltages at PCC and sequence-current injected by the BESS are shown in Fig. 18. It is evident that post-disturbance voltage recovery to pre-fault value has been confirmed in all phases. Consequently, the DVS is improved and the effects of imbalance are alleviated. Figure 18(d) designates that almost identical amount of positive-sequence current has been delivered by the BESS in all cases, while negative-sequence active current varies with unbalances. It is noticeable that Case 5 deliveres more negative-sequence current, trying to speed up the recovery procedure. As seen in Figs. 18(b) and (c), voltage regaining process is sequentially become slower in Case 1 to 5 even though BESS deliveres more power with the same order, which is due to the low voltage profile as a result of imbalance. However, the system was capable to recover the PCC voltage to 0.8 pu within 1.5s of contingency in all cases; as a result, no PV power loss will be occurred.

Figure 19 illustrates the dynamic voltage profile at PCC with D-STATCOM installed at bus 4. It can be perceived that when a D-STATCOM is installed, the system is capable to avoid any DVI in all phases. Nevertheless, Figs. 19(b) and (c) indicate that voltage retrieval speed is lower in phases B and C for the Cases 1 to 5 respectively which are expected due to reduced PV penetration. The sequence reactive current delivered by the D-STATCOM is presented in Fig. 19(d), confirming that injected positive-sequence reactive current by D-STATCOM is almost similar for all cases. However, the negative-sequence reactive current becomes zero in Cases 1 and 2 which mainly depend on the VUF. It can also be seen that PCC voltage has been recovered to 0.8 pu within 1.5s in all cases, which would ensure the uninterrupted connection of the PV systems with the grid.

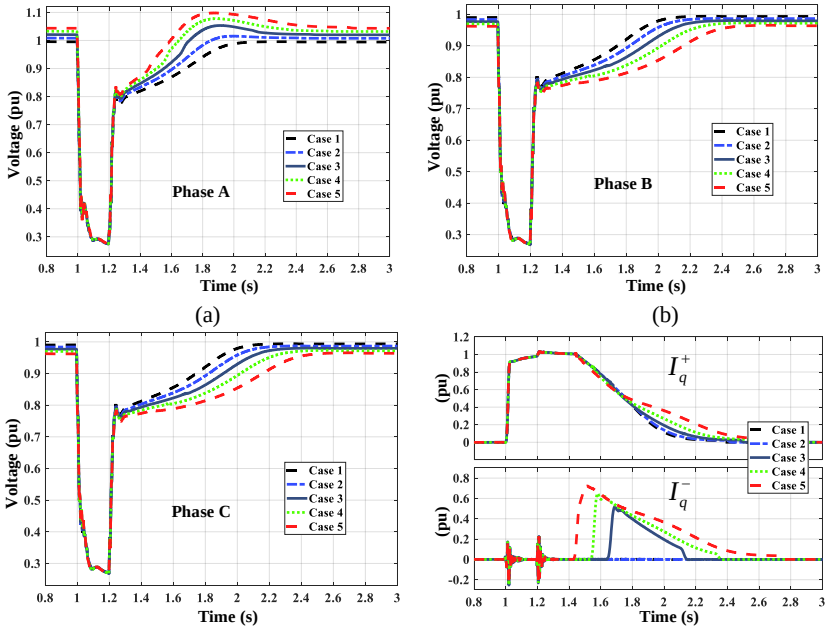

Fig 19. Dynamic voltage profile at PCC with D-STATCOM connected at bus 4: (a) Phase A (b) Phase B (c) Phase C and (d) injected positive and negative sequence reactive current.

In order to thoroughly understand the per-phase voltage dynamics, ROCOVR is calculated for the cases with BESS and D-STATCOM, and illustrated in Fig. 20. As expected, ROCOVR is improved on phase A,

while it is declining on phases B and C with the increment of imbalance for both of the scenarios. However, an interesting observation to be mentioned is that ROCOVR is less on phase B if compared with phase C in each case with the D-STATCOM. This is due to the negative-sequence current injection, attempting to reduce the unbalances. Finally, DVS in phase A is excellent, whereas although instability is mitigated, phase B and C has realized comparatively poorer DVS, respectively for the Cases 1 to 5.

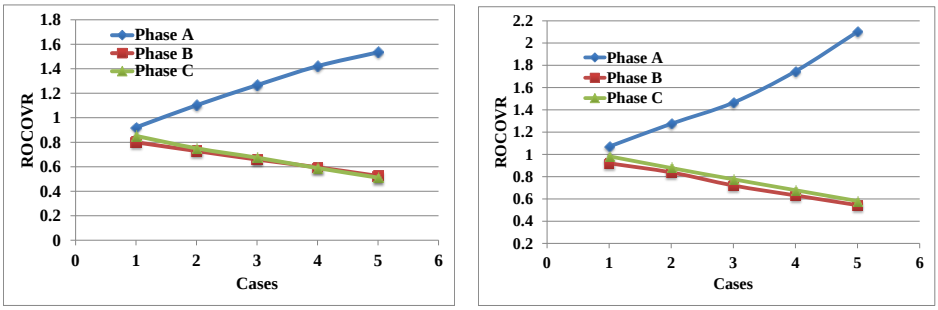

(a) (b)

Fig 20. ROCOVR for different cases with (a) BESS and (b) D-STATCOM at bus 4.

The TVSI is calculated for different cases with BESS and D-STATCOM, and tabulated in Table VII. It can be seen that TVSI gradually increases for Cases 1 to 5. As TVSI is calculated considering poorest state among three phases, it is expected a boost of TVSI for Cases 1 to 5 due to low voltage profile in phase B and C with the increase in unbalance. This phenomenon has also been observed in Figs. 18 and 19, and thus the conclusions drawn from those figures have been further validated with index. It is also evident that the TVSI in each case is high with BESS than D-STATCOM. In other words, the performance of 1000 kVA D-STATCOM in DVS improvement is better than 1000kVA BESS.

Table VII: TVSI for different cases presented in Table II with BESS and D-STATCOM.

Cases	Case 1	Case 2	Case 3	Case 4	Case 5
TVSI With BESS	646	737	960	1205	1393
TVSI With D-STATCOM	376	448	586	764	1117

*C. **Feasibility of mitigation strategies**:*

Prior discussed mitigation strategies have been compared in this section with regard to the cost and DVS improvement to emphasis on the feasibility in practical implementation. Cost comparison of the three mitigation strategies is presented in Table VIII. It may be noted that as a result of existent of roof-top PV unit in the network, additional cost for reactive-power support by roof-top PV inverters would include application of smart controller which is very insignificant. In contrast, the cost is approximately 20,000.0 AU$ for 5kVA-20kWh BESS, while it is roughly 60-65 AU$ for a 1.0 kVAr D-STATCOM [12, 68]. Therefore, the most cost-effective solution in improving the DVS of a highly PV penetrated DN would be reactive-power injection by the PV-inverters if it compared with the deployment of BESS and D-STATCOM.

Table VIII: cost comparison of mitigation strategies.

Devices	Cost
Reactive-power injection by TL-PV inverters	Insignificant
Installation of BESS	Approx. AU$ 20000.0 for 5kVA-20kWh

Installation of D-STATCOM	Approx. AU$ 300-325 for 5kVAr

In order to assess the feasibility of mitigation strategies with respect to DVS enhancement, TVSI for all three approaches are depicted in Fig. 21. It can be clearly seen that TVSI with all three mitigation strategies are less compared with no mitigation. However, implementation of reactive-power injection by TL-PV inverters have ensured lowest TVSI, whereas BESS have been realized highest TVSI among three approaches. Finally, it can be concluded that reactive-power support by PV systems would be more feasible solutions in terms of cost as well DVS improvement compared to BESS and D-STATCOM. However, to effectively use the roof-top PV units in regulation of the DN voltage, proper planning and smart control is required.

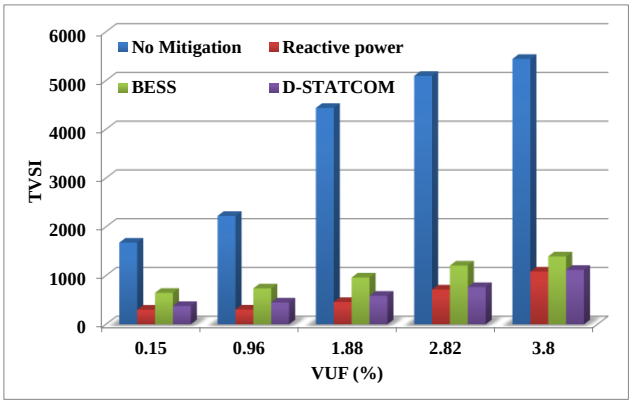

Fig 21. Comparison of TVSI for different approaches.

VI. Conclusions

As DNs are inherently unbalanced due to its unbalanced loading and unequal PV penetrations along with line characteristics, this paper has extensively investigated the impact of imbalance on the DVS of DNs, and provide solutions to mitigate a possible instability. Case studies are conducted on two benchmark IEEE test systems i.e. IEEE 4 bus and IEEE 15 bus test systems by developing dynamic model of the elements involved in the network. Provided results reveal that DVS is likely to be impaired with the increase in imbalance. It is observed that in spite of unchanged load or PV penetration on phase B, voltage instability can be occurred on this phase due to the reduction of loads or additional PV units on phase A and the opposite on phase C. Furthermore, the system was unable to recover PCC voltages to steady state condition within specified period defined in LVRT requirement in some circumstances, demanding an obligatory disconnection of the PV systems. As the system is unbalanced, to thoroughly understand the voltage dynamics in each phase, two indices i.e. voltage nadir and ROCOVR is proposed. It is observed through these indices that DVS in different phases could be non-identical. On the purpose of comparison, another index termed TVSI is also calculated for all scenarios. It has been shown that TVSI increases 253.85% and 224.95% respectively when VUF rises 0.15% to 3.08% with an unbalanced loading and 0.15% to 3.80% with unequal PV penetrations, which is the clear indication of a weaken DVS with high imbalance.

In order to alleviate the adverse effects of imbalance, three mitigation strategies: (1) reactive power injection by TL-PV systems, (2) installation of BESS and (3) D-STATCOM are suggested and compared in terms of DVS improvement and cost. It is observed that although instability can be mitigated with those approaches, phases with high or even unchanged loading still might be realized comparatively slower recovery-speed as unbalance increased. It is also perceived that reactive power support by small PV units

would be the most cost effective solutions in mitigating a probable DVI. Finally, it is expected that this study will promote awareness regarding the unseen threats of DVI in DNs among operation and planning engineers. Furthermore, to mitigate the adverse effects of imbalance on the DVS and support the network to avoid PV power loss, suggested remedial measures may be effective.

Appendix A

Table A1: Modified load of IEEE 4 bus system.

Phases	Balanced condition				
	kW		kVAr		kVA
	IM	ZIP	IM	ZIP	
A	1100	520	692	93	1800
B	1100	520	692	93	1800
C	1100	520	692	93	1800
Total	3300	1560	2076	279	5400

Table A2: pu parameters of IM load [69].

R_s	X_s	R_r	X_r	X_m	H
0.1	0.1	0.09	0.06	2.5	.28

Table A3: Modified loads of IEEE 15 bus test system.

Bus No		**2**	**3**	**4**	**5**	**6**	**7**	**8**	**9**	**10**	**11**	**12**	**13**	**14**	**15**
IM load	kW	17.85	51.0	119.3	17.85	119.3	51	119.3	51	17.85	51	17.85	119.3	119.3	51
	kVAr	11.24	32.1	65.03	11.24	65.03	32.1	65.03	32.1	11.24	32.1	11.24	65.03	65.03	32.1
ZIP load	kW	26.25	19.0	20.75	26.25	20.75	19.0	20.75	19.0	26.25	19.0	26.25	20.75	20.75	19.0
	kVAr	33.76	39.31	77.8	33.76	77.8	39.31	77.8	39.31	33.76	39.31	33.76	77.8	77.8	39.31

REFERENCES

[1] S. P. E. SPE, "Global market outlook for solar power/2019–2023."

[2] "Snapshot of global photovoltaic markets 2017, Report IEA-PVPS T1–33," IEA-PVPS2018.

[3] S. Eftekharnejad, V. Vittal, G. T. Heydt, B. Keel, and J. Loehr, "Impact of increased penetration of photovoltaic generation on power systems," *IEEE Transactions on Power Systems*, vol. 28, pp. 893-901, 2013.

[4] "Snapshot of global photovoltaic markets 2019, Report IEA-PVPS T1–35," IEA-PVPS2019.

[5] T. Han, Y. Chen, J. Ma, Y. Zhao, and Y.-Y. Chi, "Surrogate Modeling Based Multi-objective Dynamic VAR Planning Considering Short-term Voltage Stability and Transient Stability," *IEEE Transactions on Power Systems*, 2017.

[6] L. Zhu, C. Lu, Z. Y. Dong, and C. Hong, "Imbalance Learning Machine Based Power System Short-Term Voltage Stability Assessment," *IEEE Transactions on Industrial Informatics*, vol. PP, pp. 1-1, 2017.

[7] E. Nasr-Azadani, C. A. Cañizares, D. E. Olivares, and K. Bhattacharya, "Stability analysis of unbalanced distribution systems with synchronous machine and DFIG based distributed generators," *Smart Grid, IEEE Transactions on*, vol. 5, pp. 2326-2338, 2014.

[8] Y. Dong, X. Xie, C. Lu, B. Zhou, and Q. Jiang, "Local-area STVS control system," *IET Generation, Transmission & Distribution*, vol. 10, pp. 3901-3909, 2016.

[9] S. Konar, D. Chatterjee, and S. Patra, "V–Q sensitivity-based index for assessment of dynamic voltage stability of power systems," *IET Generation, Transmission & Distribution*, vol. 9, pp. 677-685, 2015.

[10] A. E. M. Operator, "Black System, South Australia, 28 September 2016," *Report of the Australian Energy Market Operator Limited (AEMO)*, 2017.

[11] B. R. Williams, W. R. Schmus, and D. C. Dawson, "Transmission voltage recovery delayed by stalled air conditioner compressors," *IEEE Transactions on Power Systems*, vol. 7, pp. 1173-1181, 1992.

[12] R. Yan and T. K. Saha, "Investigation of Voltage Stability for Residential Customers Due to High Photovoltaic Penetrations," *IEEE Transactions on Power Systems*, vol. 27, pp. 651-662, 2012.

[13] P. Kundur, J. Paserba, V. Ajjarapu, G. Andersson, A. Bose, C. Canizares, *et al.*, "Definition and classification of power system stability IEEE/CIGRE joint task force on stability terms and definitions," *IEEE transactions on Power Systems*, vol. 19, pp. 1387-1401, 2004.

[14] Z. Li, Q. Guo, H. Sun, and J. Wang, "Impact of Coupled Transmission-Distribution on Static Voltage Stability Assessment," *IEEE Transactions on Power Systems*, vol. 32, pp. 3311-3312, 2017.

[15] E. Nasr-Azadani, C. A. Cañizares, D. E. Olivares, and K. Bhattacharya, "Stability analysis of unbalanced distribution systems with synchronous machine and DFIG based distributed generators," *IEEE Transactions on Smart Grid*, vol. 5, pp. 2326-2338, 2014.

[16] G. Carpinelli, F. Mottola, D. Proto, and P. Varilone, "Minimizing unbalances in low-voltage microgrids: Optimal scheduling of distributed resources," *Applied Energy*, vol. 191, pp. 170-182, 2017.

[17] D. Q. Hung, N. Mithulananthan, and R. Bansal, "Integration of PV and BES units in commercial distribution systems considering energy loss and voltage stability," *Applied Energy*, vol. 113, pp. 1162-1170, 2014.

[18] M. Esmaili, E. C. Firozjaee, and H. A. Shayanfar, "Optimal placement of distributed generations considering voltage stability and power losses with observing voltage-related constraints," *Applied Energy*, vol. 113, pp. 1252-1260, 2014/01/01/ 2014.

[19] D. Q. Hung and N. Mithulananthan, "Loss reduction and loadability enhancement with DG: a dual-index analytical approach," *Applied Energy*, vol. 115, pp. 233-241, 2014.

[20] S. E. Sadeghi and A. Akbari Foroud, "A new approach for static voltage stability assessment in distribution networks," *International Transactions on Electrical Energy Systems*, vol. 30, p. e12203, 2020.
[21] I. G. Adebayo, A. A. Jimoh, and A. A. Yusuff, "A study of the effect of power electronic system interaction with power system voltage stability," *International Transactions on Electrical Energy Systems*, vol. 28, p. e2574, 2018.
[22] K. Kawabe and K. Tanaka, "Impact of Dynamic Behavior of Photovoltaic Power Generation Systems on Short-Term Voltage Stability," *Power Systems, IEEE Transactions on*, vol. 30, pp. 3416-3424, 2015.
[23] M. Islam, N. Mithulananthan, and M. J. Hossain, "Dynamic Behavior of Transformerless PV System on the Short-term Voltage Stability of Distribution Network " presented at the 2016 IEEE Power & Energy Society General Meeting, Chicago, USA, 2016.
[24] J. Yaghoobi, N. Mithulananthan, and T. K. Saha, "Dynamic voltage stability of distribution system with a high penetration of rooftop PV units," in *2015 IEEE Power & Energy Society General Meeting*, 2015, pp. 1-5.
[25] K. Kawabe, Y. Ota, A. Yokoyama, and K. Tanaka, "Novel Dynamic Voltage Support Capability of Photovoltaic Systems for Improvement of Short-Term Voltage Stability in Power Systems," *IEEE Transactions on Power Systems*, vol. 32, pp. 1796-1804, 2017.
[26] M. Islam, N. Mithulananthan, and M. J. Hossain, "Dynamic voltage support by TL-PV systems to mitigate short-term voltage instability in residential DN," *IEEE Transactions on Power Systems*, vol. PP, pp. 1-1, 2017.
[27] N. Afrin, F. Yang, and J. Lu, "Optimized reactive power support strategy for photovoltaic inverter to intensify the dynamic voltage stability of islanded microgrid," *International Transactions on Electrical Energy Systems*, p. e12356, 2020.
[28] D. Yang, S. Hong, H. Cheng, and L. Yao, "A novel dynamic reactive power planning methodology to enhance transient voltage stability," *International Transactions on Electrical Energy Systems*, vol. 27, p. e2390, 2017.
[29] J. Yaghoobi, M. Islam, and N. Mithulananthan, "Analytical approach to assess the loadability of unbalanced distribution grid with rooftop PV units," *Applied Energy*, vol. 211, pp. 358-367, 2018/02/01/ 2018.
[30] G. Carpinelli, P. Caramia, A. Russo, and P. Varilone, "Voltage stability in unbalanced power systems: a new complementarity constraints-based approach," *IET Generation, Transmission & Distribution*, vol. 9, pp. 2014-2023, 2015.
[31] X. Ran and S. Miao, "Probabilistic evaluation for static voltage stability for unbalanced three-phase distribution system," *IET Generation, Transmission & Distribution*, vol. 9, pp. 2050-2059, 2015.
[32] D. Schmidt, D. Siedle, and J. Ketterer, "Inverter for transforming a DC voltage into an AC current or an AC voltage," ed: EP Patent 1,369,985, 2009.
[33] M. Islam and S. Mekhilef, "Efficient Transformerless MOSFET Inverter for a Grid-Tied Photovoltaic System," *IEEE Transactions on Power Electronics*, vol. 31, pp. 6305-6316, 2016.
[34] W. Li, Y. Gu, H. Luo, W. Cui, X. He, and C. Xia, "Topology Review and Derivation Methodology of Single Phase Transformerless Photovoltaic Inverters for Leakage Current Suppression," *Industrial Electronics, IEEE Transactions on*, vol. PP, pp. 1-1, 2015.
[35] M. Victor, F. Greizer, S. Bremicker, and U. Hübler, "Method of converting a direct current voltage from a source of direct current voltage, more specifically from a photovoltaic source of direct current voltage, into a alternating current voltage," ed: United States Patents, 2008.
[36] M. Islam and S. Mekhilef, "H6-type transformerless single-phase inverter for grid-tied photovoltaic system," *IET Power Electronics*, vol. 8, pp. 636-644, 2015.
[37] R. Gonzalez, J. Lopez, P. Sanchis, and L. Marroyo, "Transformerless Inverter for Single-Phase Photovoltaic Systems," *IEEE Transactions on Power Electronics*, vol. 22, pp. 693-697, 2007.
[38] M. Ebrahimi, S. A. Khajehoddin, and M. Karimi-Ghartemani, "Fast and Robust Single-Phase DQ Current Controller for Smart Inverter Applications," *IEEE Transactions on Power Electronics*, vol. 31, pp. 3968-3976, 2016.
[39] S. Li, X. Fu, M. Ramezani, Y. Sun, and H. Won, "A novel direct-current vector control technique for single-phase inverter with L, LC and LCL filters," *Electric Power Systems Research*, vol. 125, pp. 235-244, 2015.
[40] Y. Yang, H. Wang, and F. Blaabjerg, "Reactive Power Injection Strategies for Single-Phase Photovoltaic Systems Considering Grid Requirements," *IEEE Transactions on Industry Applications*, vol. 50, pp. 4065-4076, 2014.
[41] Y. Yang, F. Blaabjerg, and H. Wang, "Low-Voltage Ride-Through of Single-Phase Transformerless Photovoltaic Inverters," *IEEE Transactions on Industry Applications*, vol. 50, pp. 1942-1952, 2014.
[42] C.-T. Lee, C.-W. Hsu, and P.-T. Cheng, "A low-voltage ride-through technique for grid-connected converters of distributed energy resources," *IEEE Transactions on Industry Applications*, vol. 47, pp. 1821-1832, 2011.
[43] R. Yan and T. K. Saha, "Investigation of voltage imbalance due to distribution network unbalanced line configurations and load levels," *IEEE Transactions on Power Systems*, vol. 28, pp. 1829-1838, 2013.
[44] A. Von Jouanne and B. Banerjee, "Assessment of voltage unbalance," *IEEE transactions on power delivery*, vol. 16, pp. 782-790, 2001.
[45] P. Gnaci, "Windings temperature and loss of life of an induction machine under voltage unbalance combined with over-or undervoltages," *IEEE Transactions on Energy Conversion*, vol. 23, pp. 363-371, 2008.
[46] "Electric Power Systems and Equipment—Voltage Ratings (60 Hertz), ANSI Standard Publication no. ANSI C84.1-1995."
[47] "Motors and Generators, NEMA Standards Publication no. MG 1-1993."
[48] Y. Xu, Z. Y. Dong, K. Meng, W. F. Yao, R. Zhang, and K. P. Wong, "Multi-objective dynamic VAR planning against short-term voltage instability using a decomposition-based evolutionary algorithm," *Power Systems, IEEE Transactions on*, vol. 29, pp. 2813-2822, 2014.
[49] K. Morison, H. Hamadani, and L. Wang, "Load modeling for voltage stability studies," in *2006 IEEE PES Power Systems Conference and Exposition*, 2006, pp. 564-568.
[50] U. Jayatunga, S. Perera, and P. Ciufo, "Voltage unbalance emission assessment in radial power systems," *IEEE Transactions on Power Delivery*, vol. 27, pp. 1653-1661, 2012.
[51] F. Ghassemi and M. Perry, "Review of voltage unbalance limit in the GB grid code CC. 6.1. 5 (b)," *National Grid, Report*, 2014.
[52] Y. Zhang, S. Ren, Z. Y. Dong, Y. Xu, K. Meng, and Y. Zheng, "Optimal placement of battery energy storage in distribution networks considering conservation voltage reduction and stochastic load composition," *IET Generation, Transmission & Distribution*, vol. 11, pp. 3862-3870, 2017.
[53] S. M. B. Sadati, J. Moshtagh, M. Shafie-khah, and J. P. Catalão, "Smart distribution system operational scheduling considering electric vehicle parking lot and demand response programs," *Electric Power Systems Research*, vol. 160, pp. 404-418, 2018.
[54] M. d. C. e Silva, A. Ferreira Filho, A. Neves, and M. Mendonça, "Effects of sequence voltage components on torque and efficiency of a three-phase induction motor," *Electric Power Systems Research*, vol. 140, pp. 942-949, 2016.
[55] C.-Y. Lee, "Effects of unbalanced voltage on the operation performance of a three-phase induction motor," *IEEE Transactions on Energy Conversion*, vol. 14, pp. 202-208, 1999.
[56] W. H. Kersting, *Distribution system modeling and analysis*: CRC press, 2012.
[57] D. Q. Hung and Y. Mishra, "Impacts of single-phase PV injection on voltage quality in 3-phase 4-wire distribution systems," in *2018 IEEE Power & Energy Society General Meeting (PESGM)*, 2018, pp. 1-5.
[58] L. Degroote, B. Renders, B. Meersman, and L. Vandevelde, "Neutral-point shifting and voltage unbalance due to single-phase DG units in low voltage distribution networks," in *2009 IEEE Bucharest PowerTech*, 2009, pp. 1-8.
[59] H. Bai and V. Ajjarapu, "A novel online load shedding strategy for mitigating fault-induced delayed voltage recovery," *IEEE Transactions on Power Systems*, vol. 26, pp. 294-304, 2011.
[60] S. M. Halpin, K. A. Harley, R. A. Jones, and L. Y. Taylor, "Slope-permissive under-voltage load shed relay for delayed voltage recovery mitigation," *IEEE Transactions on Power Systems*, vol. 23, pp. 1211-1216, 2008.
[61] M. B. Seon Gu Kim, STRI, "Towards the development of a set of grid code requirements for wind farms: Transient reactive power requirements (Part 3 Report of Vindforsk Project V-369)," 2013.

[62] T. F. Wu, C. L. Kuo, K. H. Sun, and H. C. Hsieh, "Combined Unipolar and Bipolar PWM for Current Distortion Improvement During Power Compensation," *IEEE Transactions onPower Electronics*, vol. 29, pp. 1702-1709, 2014.
[63] M. Islam, N. Afrin, and S. Mekhilef, "Efficient Single Phase Transformerless Inverter for Grid-Tied PVG System With Reactive Power Control," *IEEE Transactions on Sustainable Energy*, vol. 7, pp. 1205-1215, 2016.
[64] A. Camacho, M. Castilla, J. Miret, A. Borrell, and L. G. de Vicuña, "Active and reactive power strategies with peak current limitation for distributed generation inverters during unbalanced grid faults," *IEEE Transactions on industrial electronics*, vol. 62, pp. 1515-1525, 2015.
[65] X. Guo, X. Zhang, B. Wang, W. Wu, and J. M. Guerrero, "Asymmetrical grid fault ride-through strategy of three-phase grid-connected inverter considering network impedance impact in low-voltage grid," *IEEE Transactions on Power Electronics*, vol. 29, pp. 1064-1068, 2014.
[66] M. Islam, N. Mithulananthan, and M. J. Hossain, "A Grid-Support Strategy with PV units to Boost Short-term Voltage Stability under Asymmetrical Faults," *IEEE Transactions on Power Systems*, pp. 1-1, 2019.
[67] A. Camacho, M. Castilla, J. Miret, J. C. Vasquez, and E. Alarcón-Gallo, "Flexible voltage support control for three-phase distributed generation inverters under grid fault," *IEEE Transactions on Tndustrial Electronics*, vol. 60, pp. 1429-1441, 2013.
[68] G. He, Q. Chen, C. Kang, P. Pinson, and Q. Xia, "Optimal bidding strategy of battery storage in power markets considering performance-based regulation and battery cycle life," *IEEE Transactions on Smart Grid*, vol. 7, pp. 2359-2367, 2016.
[69] C. W. Taylor, *Power system voltage stability*: McGraw-Hill, 1994.